ADVANCED HEALTHCARE MATERIALS
www.advhealthmat.de

Silk Hydrogels Crosslinked by the Fenton Reaction

*Jaewon Choi, Meghan McGill, Nicole R. Raia, Onur Hasturk, and David L. Kaplan**

Here, the Fenton reaction is used to prepare silk hydrogels through oxidation of tyrosine residues in silk fibroin, leading to dityrosine crosslinking. At pH 5.7, gelation occurs rapidly within 30 s, and the resultant opaque gels show soft properties with a storage modulus of ≈100 Pa. The addition of ascorbic acid to the Fenton reaction increases the dityrosine bonds in the hydrogels but has little effect on the rheological or mechanical properties. The results indicate that Fe(III) ions significantly interacted with silk fibroin during the Fenton reaction, most likely binding to sites such as tyrosine, glutamate, and aspartate residues, triggering the formation of β-sheet structures that may impede dityrosine bond formation due to steric hindrance. The use of an iron chelator or the operation of the Fenton reaction at pH 9.2 enables control over the interaction of Fe(III) ions with silk fibroin, achieving a hydrogel with improved optical properties and enhanced dityrosine bond formation. Hydrogels prepared by the Fenton reaction are cytocompatible as L929 mouse fibroblasts remain viable and are proliferative when seeded on the hydrogels. The results offer a useful approach to generate chemically crosslinked silk fibroin hydrogels without the use of enzyme-catalyzed reactions for biomedical applications.

1. Introduction

Recent interest in the use of enzymes to catalyze the crosslinking of polymers and proteins has created new opportunities for injectable hydrogel systems through the development of mild enzymatic reactions similar to physiological conditions.[1,2] Among various types of enzymes, horseradish peroxidase (HRP) has been extensively used for the preparation of chemically crosslinked hydrogels, including hyaluronic acid,[3] dextran,[4] gelatin,[5] alginate,[6] chitosan,[7] and silk fibroin,[8] due to the ease of tuning the crosslinking density and gelation kinetics.[9] However, the main concern regarding the HRP-catalyzed reaction is the retention of this plant-derived enzyme in the hydrogel networks and potential immunological response in vivo.[10,11] Recently, several attempts have been made to address this limitation. For example, Bae et al. demonstrated the formation of enzyme-free hydrogels using HRP-immobilized ferromagnetic beads with a diameter of 300–500 μm. The hydrogel precursor solution was passed through a syringe packed with HRP-beads, removing enzyme from the resultant hydrogels.[12] Li et al. reported the use of HRP-immobilized porous silica particles to achieve enzyme-free dextran or gelatin hydrogels. They demonstrated that the HRP-free gelatin hydrogels showed remarkably lower levels of local and systemic inflammation than HRP-containing gels when injected subcutaneously in C57BL/6J mice.[13] In other approaches, hematin was used as an alternative catalyst to HRP for in situ formation of hydrogels[14] or was immobilized on the inner surface of a syringe to achieve hematin-free hydrogels.[15]

Silk fibroin protein, a natural biopolymer derived from the cocoons of domesticated *Bombyx mori* silkworms, has received considerable attention due to its excellent biocompatibility, controllable biodegradability, outstanding mechanical strength, and mild immunological response in vivo.[16,17] These properties make silk protein-based hydrogels suitable candidates for biomedical applications, which could overcome limitations of hydrogels prepared from conventional synthetic polymers.[18] Silk hydrogels can be prepared by physical or chemical crosslinking of silk fibroin molecules. This includes vortexing,[19] sonication,[20] pH control or high temperature,[21] electric fields,[22] and photoinitiated reactions.[23] Recently, we demonstrated the preparation of enzymatically crosslinked silk hydrogels using HRP in the presence of hydrogen peroxide (H_2O_2), where tyrosine residues in silk fibroin were covalently crosslinked and formed dityrosine bonds.[8] While these hydrogels had optical transparency, elasticity, tunable mechanical properties, and compatibility with encapsulated human mesenchymal stem cells, the retention of HRP in the hydrogels is a potential challenge related to clinical applications. Therefore, the development of a new strategy for crosslinking of silk fibroin without an enzyme was pursued to circumvent this concern.

The Fenton reaction is based on a redox pair of ferrous ion and H_2O_2 that generates a reactive hydroxyl radical ($^{\bullet}OH$). This Fenton reaction has been extensively employed as a radical initiator in the graft copolymerization of vinyl monomers onto starches, wools, celluloses, or cottons.[24] However, relatively less attention has been paid to its use for crosslinking of polymers. Recently, Barros et al. described the preparation of poly(*N*-vinyl-2-pyrrolidone) (PVP) hydrogels using the Fenton reaction, where the PVP concentration, molar ratio of $[H_2O_2]/[Fe(II)]$, and pH played important roles in the formation of hydrogels.[25] These hydrogels did not show any toxic effects on mouse

Dr. J. Choi, M. McGill, N. R. Raia, O. Hasturk, Prof. D. L. Kaplan
Department of Biomedical Engineering
Tufts University
4 Colby Street, Medford, MA 02155, USA
E-mail: david.kaplan@tufts.edu
The ORCID identification number(s) for the author(s) of this article can be found under https://doi.org/10.1002/adhm.201900644.

DOI: 10.1002/adhm.201900644

subconjunctival tissue cells or irritating effects during a dermal inflammation testing in albino rabbits. Qin et al. reported the use of citrate-modified photo-Fenton reaction to crosslink recombinant exon 1 encoded resilin.[26] More recently, Sun et al. used the Fenton reaction to generate *N*-(2-hydroxyethyl) acrylamide/poly(ethylene glycol) diacrylate hydrogels, which showed good activity of rabbit bone marrow stromal stem cells and L929 cells after encapsulation into the hydrogels.[27]

The aim of the present study was to develop a silk hydrogel system using the Fenton reaction. A number of strategies were used to improve the reaction in terms of dityrosine formation and optical clarity. Ascorbic acid was added to the Fenton reaction due to its ability to reduce Fe(III) to Fe(II), which was expected to promote the generation of •OH radicals, thereby enhancing dityrosine formation. Transparency of the hydrogels was also improved by controlling the interaction of iron ions with silk fibroin by adding an iron chelator and changing the reaction pH. The gelation time, rheological properties, compressive modulus, optical density, secondary structure, and cytocompatibility were evaluated. The approach establishes the Fenton reaction as an alternative to enzymatic crosslinking to prepare silk hydrogels for a broad range of biomedical applications.

2. Results and Discussion

2.1. Preparation of Silk Hydrogels and Characterization of Dityrosine Bonds

In the classic Fenton reaction (**Scheme 1**a), Fe(II) ion reacts with H_2O_2, generating Fe(III) ion and oxidizing •OH radical. Ascorbic acid has been used in the Fenton system to promote the generation of •OH radicals due to its ability to reduce Fe(III) to Fe(II) ion (Scheme 1b).[28] We hypothesized that the addition of ascorbic acid to Fenton reaction could increase the oxidation of tyrosine residues in silk fibroin due to an increase of the generation of •OH radicals, thereby enhancing the formation of dityrosine bonds in crosslinked hydrogels. The concentration of ascorbic acid to be added was determined by studying the pH change of the silk solution (Supporting Information, Figure S1). The pH of pristine silk solutions was 5.7, which was optically transparent. When 2.7×10^{-3} M ascorbic acid was added, the pH of the silk solutions was decreased to 4.4, and cloudiness was observed. Above 2.7×10^{-3} M ascorbic acid, the solutions showed precipitation with turbidity or underwent the sol–gel transition due to increasing inter- and intramolecular interactions, which is associated with the isoelectric point (pI = 4.39 for the N-terminus) of silk fibroin.[29] These acidic conditions could be unfavorable for the formation of dityrosine bonds owing to steric hindrance arising from the β-sheet structures, although acidic conditions (ideal pH ≈3) are preferable for Fenton reaction.[30] Consequently, lower ascorbic acid concentrations (0.4×10^{-3} and 0.8×10^{-3} M) that appeared to have little effect on the conformational change of silk fibroin were chosen for the present study.

(a) Fenton reaction

$$Fe^{2+} + H_2O_2 \longrightarrow Fe^{3+} + {}^{\bullet}OH + OH^-$$

(b) Fenton reaction with ascorbic acid

$$Fe^{2+} + H_2O_2 \longrightarrow Fe^{3+} + {}^{\bullet}OH + OH^-$$

ascorbic acid

Scheme 1. a) Fenton reaction. b) Fenton reaction in the presence of ascorbic acid, where ascorbic acid reduces Fe(III) to Fe(II) ion.

The silk hydrogels crosslinked by Fenton reaction were opaque regardless of the ascorbic acid concentration (**Figure 1**a), where their yellowish brown color is attributed to the oxidation of tyrosine residues in the presence of Fe(III) ions.[26,27,31] The hydrogel precursor solutions were instantly changed from colorless to yellowish brown upon mixing of H_2O_2 at the initiation step of crosslinking. The general mechanism of dityrosine crosslinking by Fenton reaction involves the generation of •OH radicals, followed by the oxidation of tyrosine residues to form tyrosyl radicals. Two tyrosyl radicals then couple together, leading to the formation of dityrosine bonds. The reaction products could also include 3,4-dihydroxyphenylalanine (DOPA), which is coupling of a •OH radical to a tyrosyl radical.[32]

The dityrosine bonds in the hydrogels were investigated using liquid chromatography tandem mass spectroscopy (LC-MS/MS). Figure 1b shows the chromatograms of the hydrogels formed by Fenton reaction with 0×10^{-3}, 0.4×10^{-3}, and 0.8×10^{-3} M ascorbic acid, hydrogels formed by HRP-catalyzed reaction (positive control), and sonication-induced physically crosslinked gels (negative control). Product ions for dityrosine (m/z transition = 361.1 → 315.3) were identified and quantified, where the typical retention time was 4.9 min. Dityrosine was detected in all samples except for the sonication-induced gels (negative control). As shown in Figure 1c, the maximum abundance of dityrosine was found at the enzymatically crosslinked hydrogels produced by HRP-catalyzed reaction (positive control). The control HRP hydrogels were found to have almost 21-fold greater abundance of dityrosine than that of the hydrogels produced by Fenton reaction in the absence of ascorbic acid (0×10^{-3} M ascorbic acid). A statistically significant difference in dityrosine abundance was observed between the hydrogels formed by Fenton reaction with 0.8×10^{-3} M ascorbic acid and the sonication-induced gels (negative control). This result suggests that the addition of 0.8×10^{-3} M ascorbic acid to the Fenton reaction was effective in promoting the generation of •OH radicals, leading to an increase in dityrosine bonds.

To verify further the dityrosine bonds in the hydrogels crosslinked by Fenton reaction, the hydrogels were dissolved in 9.3 M lithium bromide (LiBr) solution at 60 °C for 4 h. Since the β-sheet crystalline structures in the hydrogels can be fully dissolved in 9.3 M LiBr solution, but the dityrosine bonds cannot, this approach allows for direct assessment of the presence of the dityrosine bonds. As seen in Figure 1d, the hydrogels crosslinked by Fenton reaction with 0×10^{-3}, 0.4×10^{-3}, and 0.8×10^{-3} M ascorbic acid became optically transparent with color change from yellowish brown to brownish, indicating that the opaque property of the hydrogels are attributed to the heterogenous microstructures induced by β-sheet crystallinity.[33] For the HRP crosslinked gels (positive control), there

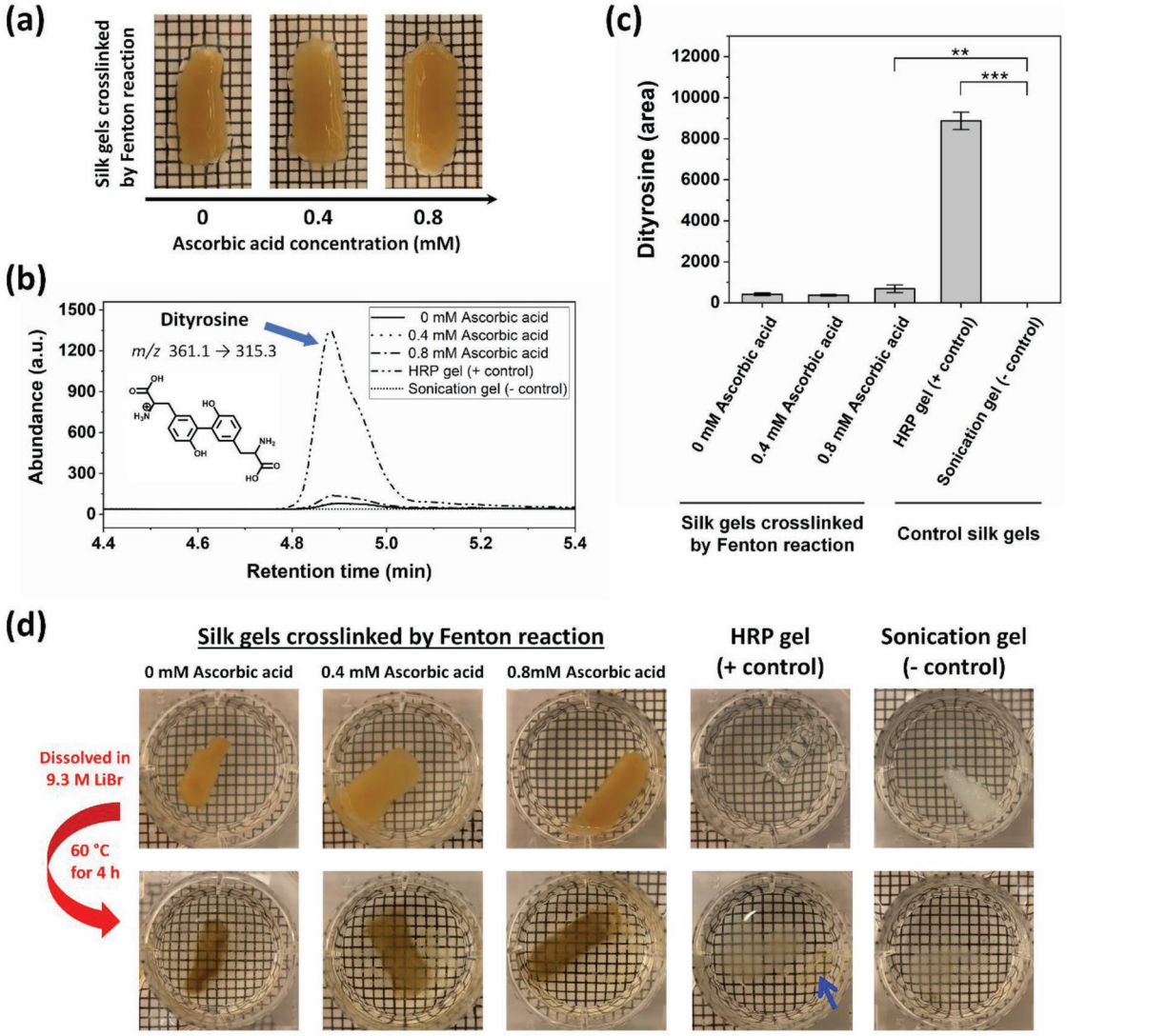

Figure 1. Silk hydrogels and analysis of dityrosine bonds. a) Photographs showing silk hydrogels (2.1% w/v) crosslinked by Fenton reaction in the absence (0×10^{-3} M) and the presence (0.4×10^{-3} and 0.8×10^{-3} M) of ascorbic acid. b) LC-MS/MS chromatograms obtained from analysis of hydrogels crosslinked by Fenton reaction with 0×10^{-3} M (solid), 0.4×10^{-3} M (dot), and 0.8×10^{-3} M (dash-dot) ascorbic acid, positive control HRP crosslinked gels (dash-dot-dot), and negative control sonication-induced physically crosslinked gels (short-dot). c) Abundance of dityrosine in peak area in the hydrogels, as determined by LC-MS/MS analysis (data are presented as mean ± standard deviation; $n = 3$, $^{**}p < 0.01$, and $^{***}p < 0.001$ by one-way ANOVA with Bonferroni post hoc test). d) Dityrosine bonds in the hydrogels were investigated by dissolving the hydrogels in 9.3 M LiBr solution at 60 °C for 4 h. Blue arrow indicates the undissolved HRP crosslinked gel. The gray substances observed at the bottom of plates in the second row are the precipitation of LiBr solution.

was a decrease in the hydrogel volume with color change to brown (blue arrow in Figure 1d). In contrast, the sonication-induced gels (negative control) were fully dissolved in 9.3 M LiBr solution, indicating the absence of the dityrosine bonds. These results are consistent with the LC-MS/MS data and confirmed the presence of the dityrosine bonds in the silk hydrogels crosslinked by Fenton reaction.

2.2. Secondary Structures of Hydrogels

The secondary structures of the hydrogels were analyzed using attenuated total reflectance-Fourier transform infrared spectroscopy (ATR-FTIR) in the amide I region (1700–1600 cm^{-1}). Generally, the bands at 1637–1616 cm^{-1} are assigned to the β-sheets.[34] The bands at 1655–1638 cm^{-1} are associated with the random coils. For Day 0 (**Figure 2**a, left), there was a band shift from ≈1620 to ≈1640 cm^{-1} when the ascorbic acid was added to Fenton reaction, suggesting the conformational change of silk fibroin from β-sheets to random coils. This result may be related to a decrease of the interaction of Fe(III) ions with silk fibroin molecules due to the reduction of Fe(III) to Fe(II) ions by the addition of ascorbic acid. As a result, the formation of β-sheet structures could be decreased or/and delayed, which will be discussed in more detail later. The β-sheet contents were 39.7 ± 5.65%, 36.2 ± 2.11%, and 36.7 ± 6.68% for

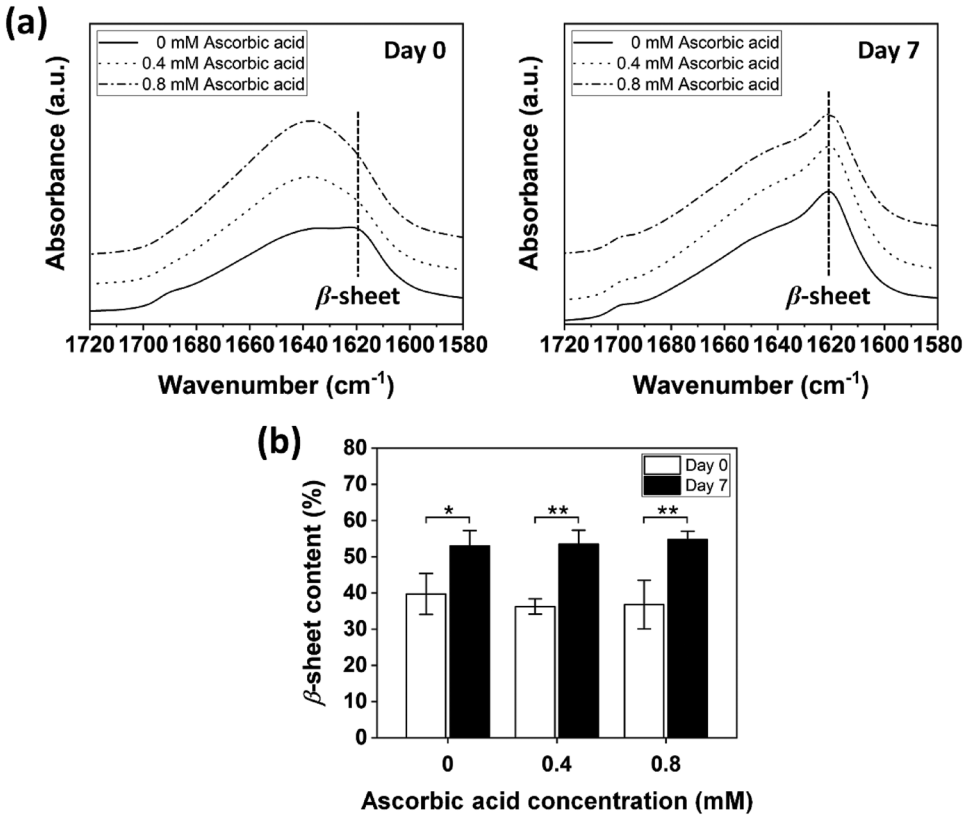

Figure 2. Representative ATR-FTIR spectra of hydrogels crosslinked by Fenton reaction with 0×10^{-3}, 0.4×10^{-3}, and 0.8×10^{-3} M ascorbic acid. a) For Day 0, a band shift was observed from ≈1620 to ≈1640 cm^{-1} when ascorbic acid was added to Fenton reaction. For Day 7, all samples showed the strong absorption band around 1620 cm^{-1}. b) β-sheet content in the hydrogels increased after incubation in PBS at 37 °C for 7 days (data are presented as mean ± standard deviation; $n = 3$, $^{*}p < 0.05$, and $^{**}p < 0.01$ by two-way ANOVA with Bonferroni post hoc test).

the samples formed with 0×10^{-3}, 0.4×10^{-3}, and 0.8×10^{-3} M ascorbic acid, respectively (Figure 2b, Day 0), where not significantly different. The distinct conformational change was observed when the hydrogels were incubated in phosphate-buffered saline (PBS, 1x) at 37 °C for 7 days (Figure 2a, right). All samples exhibited the strong absorption bands around 1620 cm^{-1} with the shoulders near 1700 cm^{-1}, and their β-sheet contents were increased to ≈53% (Figure 2b, Day 7), suggesting the formation of substantial β-sheet structures. This result is similar to the time-dependent stiffening observed in silk-based enzymatically crosslinked silk hydrogels.[35] The increased β-sheet structures in the present study could be associated with the interaction between iron ions and silk fibroin molecules, which will also be discussed in more detail later.

2.3. Rheological Properties

The gelation kinetics and mechanical properties of hydrogels were assessed through the rheological experiments at 37 °C. **Figure 3**a shows the evolution of the storage modulus (G') and loss modulus (G'') of the hydrogels formed with 0×10^{-3}, 0.4×10^{-3}, and 0.8×10^{-3} M ascorbic acid, where Fe(II), H_2O_2, and silk concentrations were held constant. When the rheological measurements began, G' was larger than G'' for all samples, indicating the dominant elastic properties at the initial time point. Qualitative observations by the vial inversion test for all samples at room temperature showed the gelation time at ≈2 min. We estimated that all hydrogel precursor solutions formed gels within 30 s as per rheological assessment. After 300 min, G' of all samples appeared to have a plateau at approximately 100 Pa (Figure 3a), regardless of the ascorbic acid concentration. The frequency sweeps (Figure 3b) showed that G' prevailed over G'' in the entire experimental range (0.1–100 rad s^{-1}) for all hydrogel samples, which is characteristic of a solid-like gel, where both G' and G'' were weakly depended on the frequency. Strain sweeps (Figure 3c) were performed to assess a critical strain of each sample. As the strain was increased beyond ≈2%, both G' and G'' began to decrease for all samples because the crosslinked network was unable to withstand applied shear deformations. Taken together, the results indicate that the hydrogels had soft properties, and the addition of ascorbic acid to Fenton reaction had no significant effect on the rheological properties of hydrogels.

2.4. Compressive Properties

Unconfined compression tests were conducted to assess the compressive properties of hydrogels. Preformed hydrogels were soaked in PBS (1x) at 37 °C and analyzed on Days 1 and 7. The samples formed with 0×10^{-3}, 0.4×10^{-3}, and 0.8×10^{-3} M

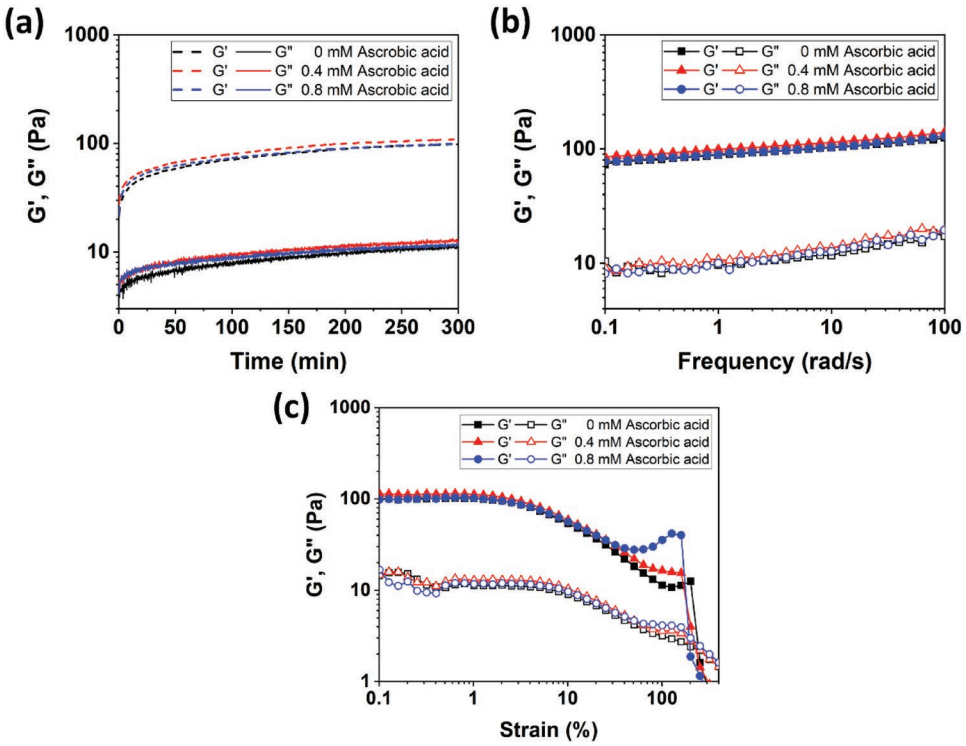

Figure 3. Representative rheological properties of hydrogels crosslinked by Fenton reaction with 0×10^{-3}, 0.4×10^{-3}, and 0.8×10^{-3} M ascorbic acid. a) Time sweeps. b) Frequency sweeps. c) Strain sweeps.

ascorbic acid showed hysteresis with permanent deformation after a single compressive loading/unloading cycle to 30% strain (**Figure 4**a). For Day 1, the compressive moduli of the samples formed with 0×10^{-3}, 0.4×10^{-3}, and 0.8×10^{-3} M ascorbic acid were 0.17, 0.11, and 0.38 kPa, respectively, where no significant differences were detected (Figure 4b). After 7 days, the samples formed with 0×10^{-3} and 0.4×10^{-3} M ascorbic acid stiffened to 1.15 and 2.29 kPa, respectively, showing increased hysteresis. This was due to the thermodynamically favorable shift in secondary structure from random coil to β-sheet over time,[36] as determined by the ATR-FTIR analysis. However, the sample formed with 0.8×10^{-3} M ascorbic acid showed a small increase in the compressive modulus from 0.38 to 0.52 kPa despite the same trend in the conformational change of silk fibroin to β-sheet structures. One of the possible reasons for this response may be related to a slightly higher abundance of dityrosine in the samples formed with 0.8×10^{-3} M ascorbic acid (Figure 1c), allowing for a delay in stiffening, however further assessments are required to confirm.

2.5. Effect of Iron Ions on Gelation of Silk Fibroin

The Fenton reaction is a very complex process, and its sequence of reaction steps is not fully understood.[30] It was hypothesized that the initiation of Fenton reaction with 1.28×10^{-3} M Fe(II) would produce equimolar Fe(III) ions (1.28×10^{-3} M) based on 1:1 mole ratio of Fe(II) to Fe(III) (Scheme 1a). To investigate the effect of iron ions on the gelation of silk fibroin, the concentration of Fe(II) or Fe(III) in silk solutions was varied in the range of 0.1×10^{-3} to 10.7×10^{-3} M, where the concentration and pH of the silk solutions were fixed at 2.3% w/v and 5.7, respectively. It should be noted that H_2O_2 was not added to the samples. **Figure 5**a shows the vial inversion tests for the samples formed with Fe(II) (left) and Fe(III) (right) after incubation at 37 °C for 1 day. For the Fe(II) ions, the silk fibroin precipitated at 1.1×10^{-3}, 1.4×10^{-3}, and 2.7×10^{-3} M, and gelled at 5.3×10^{-3} and 10.7×10^{-3} M Fe(II), forming opaque gels with a greenish color. In the case of the Fe(III) ions, gelation was observed above 0.5×10^{-3} M Fe(III) (Supporting Information, Figure S4), which is nearly one order of magnitude lower than that of Fe(II) ions. Gels containing Fe(III) ions showed an opaque yellowish brown color, which is consistent with the color of the hydrogels crosslinked by Fenton reaction (Figure 1a). This result suggests that the Fe(III) ions significantly influenced the color of the hydrogels crosslinked by Fenton reaction.

Figure 5b shows the optical density change of the samples measured at 550 nm. Results showed that the optical density increased significantly above 0.9×10^{-3} and 0.4×10^{-3} M for Fe(II) and Fe(III) ions, respectively. This is attributed to the initial formation of silk fibroin precipitates induced by Fe(II) or Fe(III) ions, followed by aggregation and gelation. The significant differences between Fe(II) and Fe(III) ions were found when iron concentration was above 0.4×10^{-3} M, except for 0.9×10^{-3} M, suggesting that the Fe(III) ions significantly affected the increase of the optical density when compared to the Fe(II) ions. These optical density changes were related to the formation of β-sheet structures (Figure 5c). For the samples containing Fe(II) or Fe(III) ions, the strong absorption bands around 1620 cm^{-1} were detected in the ATR-FTIR spectrum,

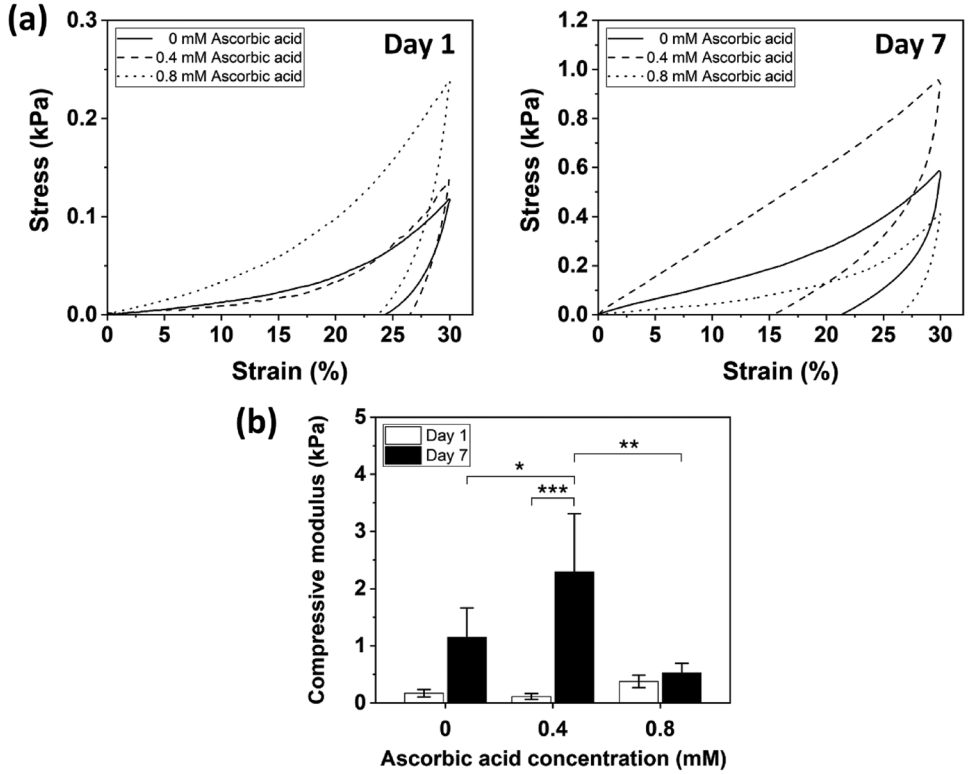

Figure 4. Representative compressive properties of hydrogels crosslinked by Fenton reaction with 0×10^{-3}, 0.4×10^{-3}, and 0.8×10^{-3} M ascorbic acid. a) Stress–strain curves showed hysteresis for both Days 1 and 7 samples. b) Compressive modulus of hydrogels. The hydrogel formed with 0.8×10^{-3} M ascorbic acid showed only a minimal increase in modulus over time (data are presented as mean ± standard deviation; $n = 5$, $^{*}p < 0.05$ and $^{**}p < 0.01$ by two-way ANOVA with Tukey's post hoc test, and $^{***}p < 0.001$ by two-way ANOVA with Bonferroni post hoc test).

which is characteristic of β-sheets. This result suggests that both Fe(II) and Fe(III) ions affected the conformational change of silk fibroin to β-sheet structures if their concentration was above a critical value, thereby forming heterogenous microstructures that cause light scattering in the range of visible light.[33] Based on these findings, it appears that Fe(III) ions more strongly interact with silk fibroin through binding sites, such as tyrosine, glutamate, and aspartate residues,[37–39] when compared to Fe(II) ions, triggering the formation of β-sheet structures and further accelerating the sol–gel transition during Fenton reaction. Therefore, the formation of dityrosine bonds could be hindered by steric hindrance arising from the preformed β-sheet structures.[40]

2.6. Optically Transparent Hydrogels and Proposed Mechanism of Silk Hydrogels Crosslinked by Fenton Reaction

We hypothesized that decreasing the interaction of Fe(III) ions with silk fibroin during the Fenton reaction could reduce the formation of heterogenous microstructures that cause light scattering, enabling us to achieve an optically transparent hydrogel. To this end, two different approaches were used: 1) the addition of ethylenediaminetetraacetic acid (EDTA), an iron chelator, and 2) the operation of Fenton reaction at pH 9.2. In both cases, Fe(II), H_2O_2, and silk concentrations were held constant. The hydrogels formed at pH 5.7 (**Figure 6**a, left) showed an opaque yellowish brown color, as described above. Notably, the hydrogels formed with EDTA at pH 5.7 (Figure 6a, middle) and at pH 9.2 (Figure 6a, right) were optically semitransparent and transparent, respectively, suggesting a decrease of heterogenous microstructures.

The maximum abundance of dityrosine was found in the optically transparent hydrogels prepared at pH 9.2 and was significantly higher than pH 5.7 and EDTA gels (Figure 6b). When pH of silk solution is above 9, the silk fibroin will be negatively charged due to the deprotonation of the acidic groups, resulting in more extended chain conformation arising from electrostatic repulsion.[41] In this case, the formation of β-sheet structures triggered by Fe(III) ions, which cause light scattering, could be effectively suppressed due to strong repulsive force among silk fibroin molecules. Additionally, buried tyrosine residues, which are located in both hydrophobic (about 70% of tyrosine residues) and hydrophilic regions of silk fibroin,[31] could be exposed to the reaction medium and enhance dityrosine crosslinking. However, a much longer gelation time (≈2 days) was observed at pH 9.2 when compared to the hydrogels formed at pH 5.7 (≈30 s). One possible reason for such behavior could be attributed to a decrease in the activity of Fenton reaction at higher pH.[30]

The abundance of dityrosine in the hydrogels formed with EDTA at pH 5.7 was lower than that of the hydrogels formed at pH 5.7 (Figure 6b). EDTA is an iron chelator, which binds both Fe(II) and Fe(III), and in particular has higher affinity for

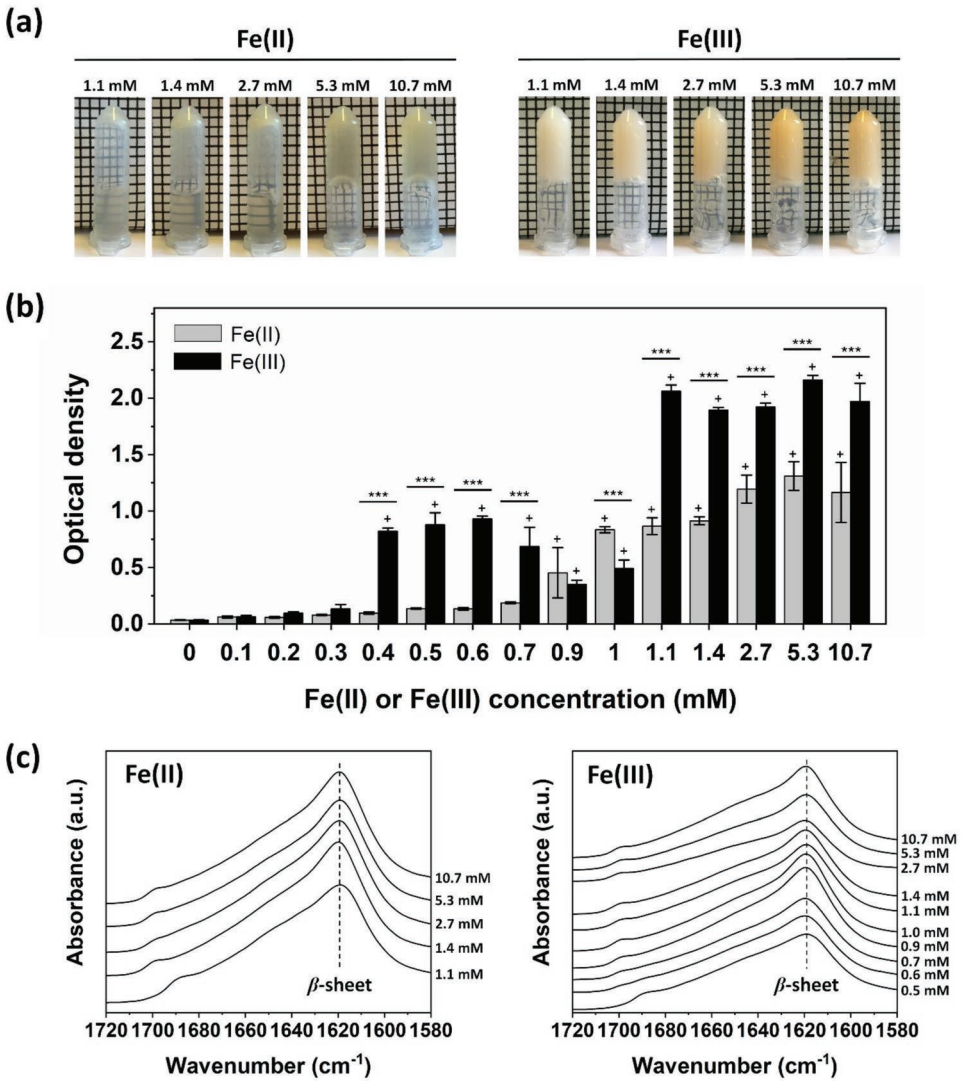

Figure 5. Effect of iron ions on gelation of silk fibroin at pH 5.7. a) Photographs showing the gelation of silk fibroin triggered by Fe(II) (left) or Fe(III) ions (right) after incubation at 37 °C for 1 day. Gels containing Fe(II) ions showed an opaque greenish color, whereas gels containing Fe(III) ions showed an opaque yellowish brown color. b) Samples containing Fe(II) or Fe(III) ions in the range of 0.1×10^{-3} to 10.7×10^{-3} M showed increased optical density as iron concentration was increased (data are presented as mean ± standard deviation; $n = 3$, $^{+}p < 0.001$ compared to 0×10^{-3} M Fe(II) or Fe(III), and $^{***}p < 0.001$ by two-way ANOVA with Bonferroni post hoc test). c) ATR-FTIR spectra of the samples formed with Fe(II) (left) or Fe(III) (right) ions showed strong absorption bands around 1620 cm^{-1}.

Fe(III) ions.[42] As expected, the addition of EDTA to Fenton reaction could result in the formation of Fe(II)–EDTA complexes, which decreases available Fe(II) ions that react with H_2O_2 to generate $^{\bullet}OH$ radicals.[43] As a result, the oxidation of tyrosine residues was decreased, resulting in lower formation of dityrosine in the hydrogels. In spite of this, a possible reason for the optically semitransparent property is that Fe(III) ions could be sequestered to a certain extent by forming Fe(III)–EDTA complexes, reducing the interaction of Fe(III) ions with silk fibroin. Furthermore, this result may explain the conformational shift of silk fibroin from β-sheets to random coils when ascorbic acid was added to Fenton reaction (Figure 2a, Day 0). Since the ascorbic acid reduced Fe(III) to Fe(II) ions, the interaction of Fe(III) ions with silk fibroin was reduced, resulting in a decrease in the formation of β-sheet structures.

It is noted that no precipitation arising from insoluble $Fe(OH)_3$ was visually observed in the optically semitransparent (Figure 6a, middle) and transparent hydrogels (Figure 6a, right). This may be related to the binding effect of Fe(III) ions to both EDTA and silk fibroin (Figure 6a, middle) and to silk fibroin (Figure 6a, right), thereby inhibiting the formation of insoluble $Fe(OH)_3$. The hydrogel precursor solutions without EDTA at pH 5.7 showed instant color change to yellowish brown upon mixing with H_2O_2, whereas the solutions containing EDTA at pH 5.7 did not show instant color change, suggesting rapid sequestration of product Fe(III) ions from Fenton reaction by EDTA at the initiation step of crosslinking. This result indicates that initial color change of the hydrogel precursor solutions could be attributed to the generation of Fe(III) ions rather than the oxidation of tyrosine residues. Overall, these findings confirm

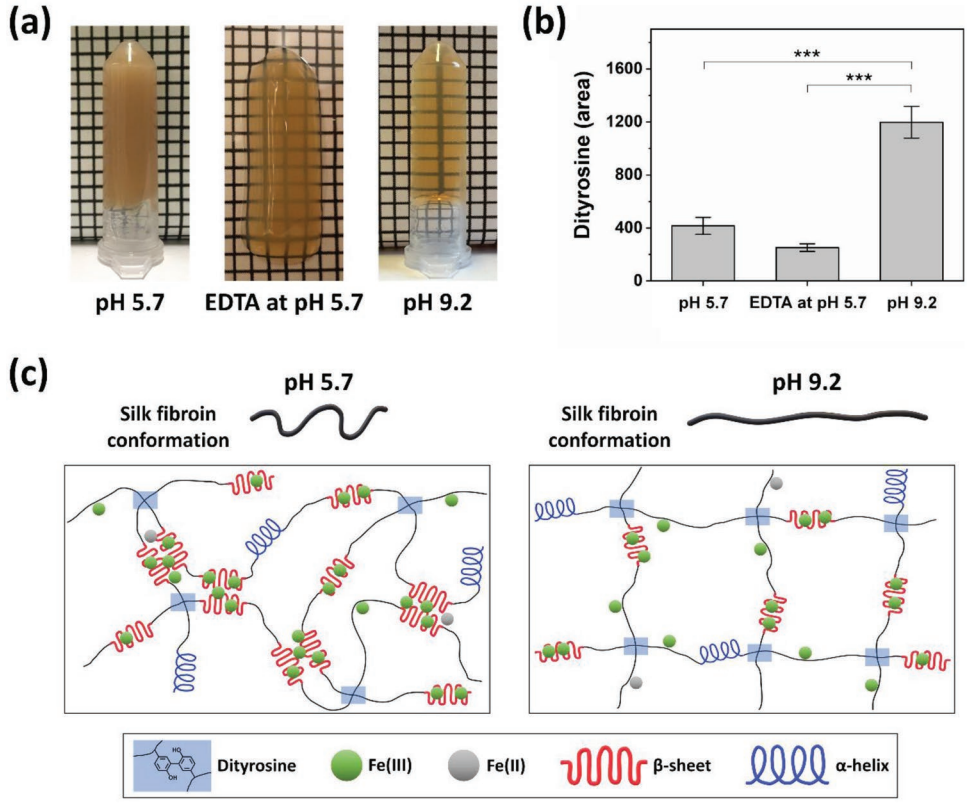

Figure 6. a) Hydrogels formed by Fenton reaction at pH 5.7 (left), with EDTA at pH 5.7 (middle), and at pH 9.2 (right) were opaque, optically semi-transparent, and transparent, respectively. b) Abundance of dityrosine in peak area in the hydrogels, as determined by LC-MS/MS analysis, shows that hydrogels at pH of 9.2 exhibited the highest dityrosine abundance (data are presented as mean ± standard deviation; $n = 3$, $^{***}p < 0.001$ by one-way ANOVA with Tukey's post hoc test). c) Proposed mechanism of silk hydrogels crosslinked by Fenton reaction. At pH 5.7 (left), Fe(III) ions, which are bound to tyrosine, glutamate, and aspartate residues, readily trigger the formation of β-sheet structures due to the less extended and compressed chain conformation of silk fibroin, hindering dityrosine crosslinking. At pH 9.2 (right), silk fibroin has more extended chain conformation due to electrostatic repulsion, suppressing the formation of β-sheet structures triggered by Fe(III) ions and allowing tyrosine residues to overcome the steric hindrance by β-sheet structures. This enhanced dityrosine formation.

the above hypothesis, and suggest that control over Fe(III) ions in the Fenton reaction is important to achieve a transparent hydrogel with enhanced dityrosine bonds. Optically transparent silk hydrogels could be used as a scaffolding material for ophthalmic applications, specifically in cornea replacements[44,45] or for optical sensing and diagnostic applications.[46,47]

Figure 6c shows the schematic illustration of the proposed mechanism of silk hydrogels crosslinked by Fenton reaction. Between Fe(II) and Fe(III) ions, the Fe(III) ions played important roles in dityrosine crosslinking of silk fibroin during Fenton reaction. Once the Fenton reaction was initiated, there was likely rapid binding of Fe(III) ions to silk fibroin through electrostatic interactions with tyrosine, glutamate, and aspartate residues.[37–39] We hypothesize that this Fe(III) binding process was much faster than the oxidation of tyrosine residues. At pH 5.7 (Figure 6c, left), the less extended and compressed chain conformation of silk fibroin would allow Fe(III) ions to readily trigger the formation of β-sheet structures through hydrophobic interactions and further induce the sol–gel transition of silk fibroin with formation of heterogenous microstructures that cause light scattering. As a result, the interaction between tyrosyl radicals for dityrosine formation was most likely sterically hindered due to the predominant β-sheet structures,[40] resulting in less dityrosine bonds, as evidenced from the LC-MS/MS data. At pH 9.2 (Figure 6c, right), the silk fibroin molecules had more extended chain conformation than those at pH 5.7 due to electrostatic repulsive force. This chain conformation could suppress the acceleration of β-sheet formation even though Fe(III) ions bound to silk fibroin, and allow tyrosine residues to overcome the steric hindrance arising from β-sheet structures. Despite a decrease in the activity of Fenton reaction at pH 9.2, which generates fewer $^{\bullet}$OH radicals, the extended chain conformation of silk fibroin resulted in greater dityrosine bonds, as confirmed by the LC-MS/MS analysis.

2.7. Cell Viability

To evaluate the cytocompatibility of silk hydrogels crosslinked by Fenton reaction, L929 mouse fibroblast cells were cultured on the surface of preformed gels (**Figure 7**a). Live/dead staining of the cells seeded on the gels produced by Fenton reaction showed high cell viability and proliferation with negligible cell death over 7 days, similar to that of HRP crosslinked gels and tissue culture plastic (TCP) controls, indicating the cytocompatibility of the hydrogels formed by Fenton reaction. It is noted that the cells cultured on

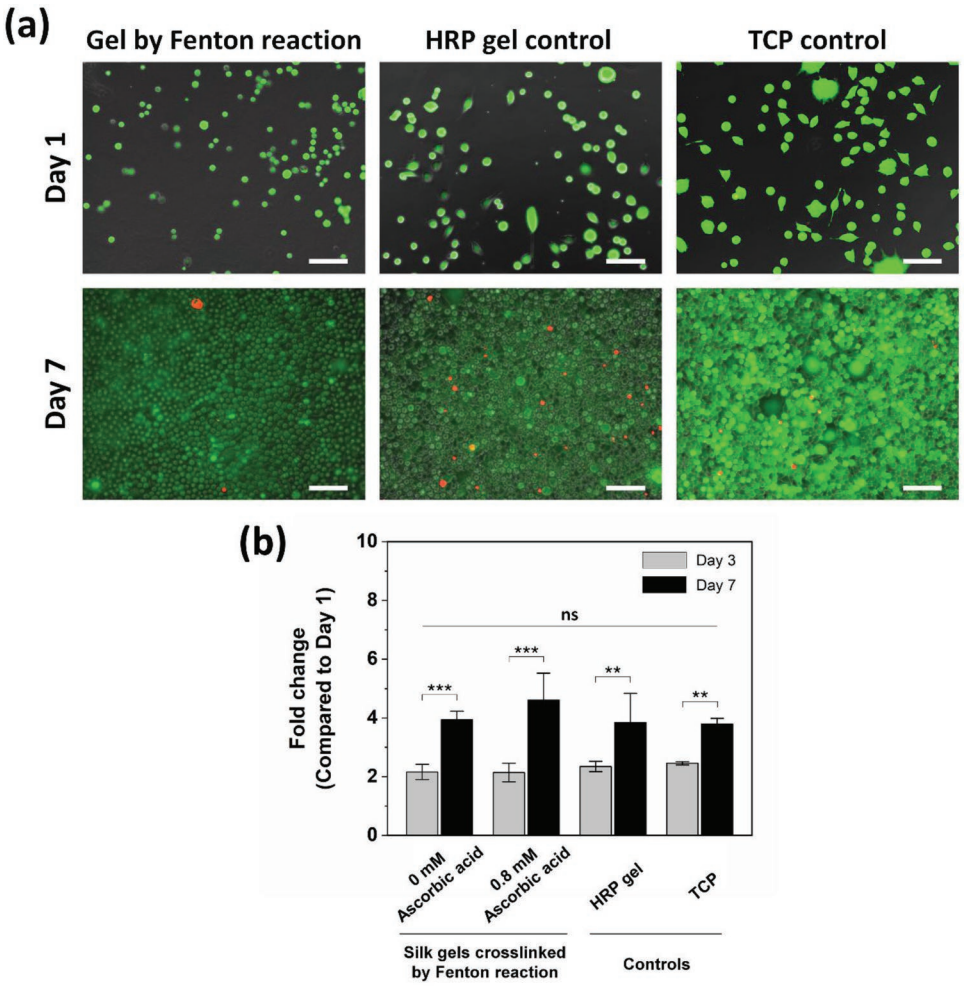

Figure 7. L929 cell viability. a) Fluorescence images of live (green) and dead (red) L929 mouse fibroblasts cultured in 2D indicated high cell viability with minimal cell death. Scale bars: 100 µm. b) Cell proliferation on silk gels formed by Fenton reaction over a 7 day period, as determined by Alamar Blue assay. Fold change in metabolic activity was calculated for Days 3 and 7, as compared to Day 1 (data are presented as mean ± standard deviation; $n = 4$, $^{**}p < 0.01$, and $^{***}p < 0.001$ by two-way ANOVA with Bonferroni post hoc test, ns = not significant).

the surface of the hydrogels crosslinked by Fenton reaction were embedded within the hydrogels over time (Supporting Information, Figure S5). The viability and proliferation were further evaluated by assessing the metabolic activity of the cells through Alamar Blue assay (Figure 7b). For 7 days, an average fold change of 3.9, 4.6, 3.8, and 3.8 in metabolic activity was detected on the hydrogels formed by Fenton reaction in the absence of ascorbic acid (0×10^{-3} M ascorbic acid), with 0.8×10^{-3} M ascorbic acid, HRP crosslinked gels, and TCP controls, respectively. No significant differences in the metabolic activity between the gels formed by Fenton reaction and control samples were observed. This result indicates that silk hydrogels crosslinked by Fenton reaction in the absence or presence of ascorbic acid are cytocompatible and viable substrates for cell growth.

3. Conclusion

In summary, the present study describes the preparation of silk hydrogels via dityrosine crosslinking using Fenton reaction. Although further studies are necessary to elucidate the relationship between iron ions and silk fibroin molecules, our findings hint at the use of Fenton reaction to create a silk hydrogel system for biomedical applications, while overcoming the potential concerns (e.g., immunological response) with enzymatically crosslinked hydrogels. Furthermore, the approach presented here could be extended in a number of ways, including: 1) the preparation of enzyme-free hydrogels, 2) other protein-based hydrogels such as sericin-based systems or if the protein has intrinsic tyrosine residues or phenolic hydroxyl moieties that can be introduced through chemical reactions, and 3) silk composite hydrogels if a counterpart polymer has phenolic hydroxyl moieties.

4. Experimental Section

Preparation of Aqueous Silk Solutions: Aqueous silk fibroin solutions were prepared using an established protocol.[48] Briefly, 5 g of cut cocoons of *B. mori* silkworms were boiled in 2 L of 0.02 M sodium carbonate (Na_2CO_3, Sigma-Aldrich, St. Louis, MO) solution for 30 min

to extract the silk fibroin protein and remove the sericin. The extracted silk fibers were rinsed with deionized (DI) water three times and dried in a fume hood overnight. The dried fibers were dissolved in 9.3 M LiBr (Sigma-Aldrich, St. Louis, MO) solution at 60 °C for 4 h. The silk solution was then dialyzed against DI water using standard grade regenerated cellulose dialysis membrane (MWCO: 3500 kD, Spectra/Por3 Standard RC Tubing, Spectrum Laboratories Inc., Rancho Dominguez, CA) for 3 days with six changes of DI water. The silk solution was then centrifuged twice (9000 RPM, 4 °C, 20 min) to remove impurities. The concentration of resulting silk solutions was ≈6–7% w/v, which was determined by weighing the mass of a dried sample after drying a known volume of aqueous silk solution at 60 °C overnight.

Preparation of Crosslinked Silk Hydrogels: Silk hydrogels were prepared by crosslinking the tyrosine residues present in silk fibroin using the Fenton reaction. Iron(II) chloride tetrahydrate ($FeCl_2{\cdot}4H_2O$, 99.99%, Sigma-Aldrich, St. Louis, MO) was dissolved in UltraPure distilled water (Thermo Fisher Scientific, Waltham, MA) to prepare 13.3×10^{-3} M Fe(II) solution. Hydrogen peroxide (H_2O_2, 30% w/w, Sigma-Aldrich, St. Louis, MO) was mixed with UltraPure distilled water to prepare 337×10^{-3} M H_2O_2 solution. Ascorbic acid solutions (3.7×10^{-3} and 8.5×10^{-3} M) were prepared from L-ascorbic acid (≥99.0%, Sigma-Aldrich, St. Louis, MO) and UltraPure distilled water. Crosslinking was initiated by adding 152 µL of 13.3×10^{-3} M Fe(II) solution followed by adding 152 µL of 337×10^{-3} M H_2O_2 solution to 1272 µL of silk solution (pH 5.7) with gentle pipetting, where the total volume of the mixture was fixed at 1576 µL (final concentration of 1.28×10^{-3} M Fe(II), 32.5×10^{-3} M H_2O_2, and 2.1% w/v silk solution). The samples were allowed to incubate at 37 °C for 4 h. At pH 9.2, the hydrogels were prepared under the same conditions except the pH of the silk solution was adjusted by addition of 1 M sodium hydroxide (NaOH) solution.

To investigate the effect of ascorbic acid on the Fenton reaction, 152 µL of 3.7×10^{-3} or 8.5×10^{-3} M ascorbic acid solution was added to 1120 µL of silk solution (pH 5.7), followed by adding 152 µL of 13.3×10^{-3} M Fe(II) solution. Crosslinking was initiated by adding 152 µL of 337×10^{-3} M H_2O_2 solution to the mixture solution with gentle pipetting, where the total volume of the solution was fixed at 1576 µL (final concentration of 1.28×10^{-3} M Fe(II), 0.4×10^{-3} or 0.8×10^{-3} M ascorbic acid, 32.5×10^{-3} M H_2O_2, and 2.1% w/v silk solution). The samples were allowed to incubate at 37 °C for 4 h. As a positive control, enzymatically crosslinked silk hydrogels with same concentration of silk solution (2.1% w/v) as that of the hydrogels formed by the Fenton reaction were prepared via HRP (type VI, Sigma-Aldrich) catalyzed reaction. Briefly, 10 µL of 1000 U mL^{-1} stock solution of HRP and 10 µL of 164×10^{-3} M H_2O_2 solution were added to 1 mL of 2.1% w/v silk solution (final concentration of 10 U mL^{-1} HRP and 1.64×10^{-3} M H_2O_2). The samples were then allowed to incubate at 37 °C for 4 h. As a negative control, physically crosslinked silk hydrogels formed via sonication were prepared. Briefly, 1 mL of 2.1% w/v silk solution in 2 mL Eppendorf tube was sonicated at 15% amplitude for 40 s using a sonifier (Branson Ultrasonics, Danbury, CT), which consisted of the Model 450 power supply, converter, externally threaded disruptor horn, and 1/8" (3.175×10^{-3} M) diameter-tapered microtip. After sonication, the samples were allowed to incubate at 37 °C for 4 h. To assess the effect of iron chelators on Fenton reaction, 152 µL of 13.3×10^{-3} M EDTA solution prepared from solutioethylenediaminetetraacetic acid (EDTA) disodium salt ($C_{10}H_{14}N_2Na_2O_8{\cdot}2H_2O$, Sigma Grade, plant cell culture tested, 98.5–101.5%, Sigma-Aldrich, St. Louis, MO) and UltraPure distilled water was added to 1120 µL of silk solution (pH 5.7), followed by adding 152 µL of 13.3×10^{-3} M Fe(II) solution. The molar ratio of EDTA to Fe(II) was fixed at 1:1. Crosslinking was initiated by adding 152 µL of 337×10^{-3} M H_2O_2 solution to the mixture solution with gentle pipetting, where the total volume of the solution was fixed at 1576 µL (final concentration of 1.28×10^{-3} M Fe(II), 1.28×10^{-3} M EDTA, 32.5×10^{-3} M H_2O_2, and 2.1% w/v silk solution). The samples were allowed to incubate at 37 °C for 4 h.

LC-MS/MS: Silk hydrogels (1 mL) were incubated with 1 mL of 12 M hydrochloric acid (HCl, 37%, Sigma-Aldrich, St. Louis, MO) at 60 °C for 8 h. The hydrolyzed samples were dehydrated at 90 °C overnight using a digital dry heat bath (Model: BSH1002, USA Scientific, Ocala, FL). The samples were then reconstituted in 1 mL of 75% v/v LC-MS grade acetonitrile in LC-MS grade water (both Fisher Scientific, Waltham, MA) and then diluted with 75% v/v LC-MS grade acetonitrile in LC-MS grade water to a final concentration of 400 µg mL^{-1}. LC-MS/MS analysis was performed according to the previously described method to detect dityrosine.[49]

ATR-FTIR: Secondary structures of hydrogels were investigated using a JASCO FTIR 6200 spectrometer (JASCO, Tokyo, Japan) with a MIRacle attenuated total reflectance (ATR) with germanium crystal. Data were obtained by averaging 32 scans with a resolution of 4 cm^{-1} within the wavenumber range of 600 and 4000 cm^{-1}. Day 0 samples were allowed to gel at 37 °C for 4 h prior to analysis. Day 7 samples were allowed to incubate in Dulbecco's PBS (DPBS, 1x, Thermo Fisher Scientific, Waltham, MA) at 37 °C for 7 days prior to analysis. Each sample was washed in deuterated water (Sigma-Aldrich, St. Louis, MO) three times for 30 min prior to the measurements to remove the interference of water in the amide I region (1700–1600 cm^{-1}). Data analysis was performed using the Fourier self-deconvolution method in the Origin Software (OriginPro 2018, OriginLab, Northampton, MA).

Rheology: Rheological measurements were performed on a TA Instruments ARES-LS2 rheometer (TA Instruments, New Castle, DE) using a 25 mm stainless steel cone (angle: 0.0994 rad) and a temperature controlled Peltier plate at 37 °C. An 800 µL aliquot of the sample was loaded onto the plate. The cone was then lowered to a gap of 0.047 in. The excess sample from the edge of the cone was removed, and silicone oil was placed around the cone to prevent water evaporation during the measurements. The dynamic time sweeps were carried out at 6.283 rad s^{-1} (1 Hz) with 1% strain for 300 min. Following gelation, dynamic frequency sweeps (0.1–100 rad s^{-1} at 1% strain) and strain sweeps (0.1–500% at 6.283 rad s^{-1} (1 Hz)) were performed. Rheological measurements were carried out in the linear viscoelastic region, where the storage modulus was independent of the applied strain.

Compression Test: Unconfined compression tests were performed on an Instron 3366 universal testing system (Instron, Norwood, MA). Preformed hydrogels (≈8 mm in diameter and ≈4 mm in height) were loaded between stainless steel parallel plates. The upper plate was then lowered until a compression force of ≈0.002 N to ensure full contact. A single compressive loading/unloading cycle to 30% strain at 0.02% s^{-1} was then performed. Prior to the test, the hydrogels were incubated in PBS (1x) at 37 °C for 1 day and 7 days. Compressive modulus was calculated for each sample as the slope between 5% and 10% strain.

Optical Density Change: $FeCl_3$ (Iron(III) chloride, 97%, Sigma-Aldrich, St. Louis, MO) solutions were prepared at the following concentrations: 1×10^{-3}, 2×10^{-3}, 3×10^{-3}, 4×10^{-3}, 5×10^{-3}, 6×10^{-3}, 7×10^{-3}, 8×10^{-3}, 9×10^{-3}, 10×10^{-3}, 13.3×10^{-3}, 25×10^{-3}, 50×10^{-3}, or 100×10^{-3} M. Then, 152 µL of Fe(III) solution was added to 1272 µL of silk solution with gentle pipetting, where the total volume of the mixture was fixed at 1424 µL (final concentration of 0.1×10^{-3}, 0.2×10^{-3}, 0.3×10^{-3}, 0.4×10^{-3}, 0.5×10^{-3}, 0.6×10^{-3}, 0.7×10^{-3}, 0.9×10^{-3}, 1×10^{-3}, 1.1×10^{-3}, 1.4×10^{-3}, 2.7×10^{-3}, 5.3×10^{-3}, or 10.7×10^{-3} M Fe(III) and 2.3% w/v silk solution). A 300 µL aliquot of the silk solution containing Fe(III) was immediately loaded into 96 well plates (MICROTEST 96, Falcon, USA) and allowed to incubate at 37 °C for 1 day. Optical density change of the samples was monitored at 550 nm using a SpectraMax M2 multi-mode microplate reader (Molecular Devices, Sunnyvale, CA). $FeCl_2$ samples were investigated in the same manner as the $FeCl_3$ experiments.

Cell Survival and Proliferation: L929 mouse fibroblast cells were cultured in growth media composed of Dulbecco's Modified Eagle Medium (DMEM, Gibco) supplemented with 10% fetal bovine serum and 1% penicillin-streptomycin (Life Technologies, Carlsbad, CA). For sterilization, silk solutions were filtered with 0.22 µm syringe filter unit (polyvinylidene difluoride membrane, MillexGV, Millipore). Cells at passage 7 were seeded on the surface of preformed silk gels (≈11 mm in diameter and ≈2.5 mm in height) prepared by Fenton reaction in the absence of ascorbic acid, Fenton reaction with 0.8×10^{-3} M ascorbic acid, gel controls crosslinked using HRP, and TCP controls at a density of 8000 cells cm^{-2}. The media was changed every 3 days. The viability of

cells was investigated using LIVE/DEAD Cell Imaging Kit (Invitrogen by Thermo Fisher Scientific) after being cultured for 1, 3, and 7 days. Samples were imaged using a BZ-X700 Fluorescence Microscope (Keyence Corp., Itasca, IL). Metabolic activity at Days 1, 3, and 7 was determined using Alamar Blue assay by incubating cells in 500 µL dye solution (10% v/v in DMEM high glucose colorless (Gibco) solution) for 2 h at 37 °C and 5% CO_2. Absorbance was measured at 570 nm (reduced) and 595 nm (oxidized) using a SpectraMax M2 multi-mode microplate reader (Molecular Devices, Sunnyvale, CA). Dye reduction (%) was calculated as described in the assay guidance manual. Blank TCP and acellular hydrogels were used to adjust for background absorbance.

Statistical Analysis: LC-MS/MS, ATR-FTIR, rheological analysis, and optical density change analysis were carried out on $n = 3$ independent sample replicates at each condition. Metabolic activity analysis was carried out on $n = 4$ independent sample replicates at each condition. Compression tests were carried out on $n = 5$ independent sample replicates at each condition. Average values and standard deviations were calculated and used to generate graphical figures. One- or two-way analysis of variance (ANOVA) with Tukey's or Bonferroni post hoc test were performed using GraphPad prism (GraphPad Software, San Diego, CA) to determine statistical significance ($^{*}p < 0.05$, $^{**}p < 0.01$, $^{***}p < 0.001$).

Supporting Information

Supporting Information is available from the Wiley Online Library or from the author.

Acknowledgements

This work was supported by the Air Force Office of Scientific Research (FA9550-17-1-0333) and the National Institutes of Health (R01EB021264 and R01AR070975).

Conflict of Interest

The authors declare no conflict of interest.

Keywords

crosslinking, dityrosine, Fenton reaction, hydrogels, silk fibroin

Received: May 21, 2019
Revised: July 3, 2019
Published online: July 25, 2019

[1] L. S. Moreira Teixeira, J. Feijen, C. A. van Blitterswijk, P. J. Dijkstra, M. Karperien, *Biomaterials* **2012**, *33*, 1281.
[2] N. E. Davis, S. Ding, R. E. Forster, D. M. Pinkas, A. E. Barron, *Biomaterials* **2010**, *31*, 7288.
[3] M. Kurisawa, J. E. Chung, Y. Y. Yang, S. J. Gao, H. Uyama, *Chem. Commun.* **2005**, 4312.
[4] R. Jin, C. Hiemstra, Z. Zhong, J. Feijen, *Biomaterials* **2007**, *28*, 2791.
[5] M. Hu, M. Kurisawa, R. Deng, C.-M. Teo, A. Schumacher, Y.-X. Thong, L. Wang, K. M. Schumacher, J. Y. Ying, *Biomaterials* **2009**, *30*, 3523.
[6] S. Sakai, K. Kawakami, *Acta Biomater.* **2007**, *3*, 495.
[7] R. Jin, L. S. M. Teixeira, P. J. Dijkstra, M. Karperien, C. A. van Blitterswijk, Z. Y. Zhong, J. Feijen, *Biomaterials* **2009**, *30*, 2544.
[8] B. P. Partlow, C. W. Hanna, J. Rnjak-Kovacina, J. E. Moreau, M. B. Applegate, K. A. Burke, B. Marelli, A. N. Mitropoulos, F. G. Omenetto, D. L. Kaplan, *Adv. Funct. Mater.* **2014**, *24*, 4615.
[9] F. Lee, J. E. Chung, M. Kurisawa, *Soft Matter* **2008**, *4*, 880.
[10] T. Sminia, F. Delemarre, E. M. Janse, *Immunology* **1983**, *50*, 53.
[11] F. Lee, K. H. Bae, M. Kurisawa, *Biomed. Mater.* **2016**, *11*, 014101.
[12] J. W. Bae, B. Y. Kim, E. Lih, J. H. Choi, Y. Lee, K. D. Park, *Chem. Commun.* **2014**, *50*, 13710.
[13] L. Li, K. H. Bae, S. Ng, A. Yamashita, M. Kurisawa, *Acta Biomater.* **2018**, *81*, 103.
[14] S. Sakai, K. Moriyama, K. Taguchi, K. Kawakami, *Biomacromolecules* **2010**, *11*, 2179.
[15] E. Byun, J. H. Ryu, H. Lee, *Chem. Commun.* **2014**, *50*, 2869.
[16] L. Meinel, S. Hofmann, V. Karageorgiou, C. Kirker-Head, J. McCool, G. Gronowicz, L. Zichner, R. Langer, G. Vunjak-Novakovic, D. L. Kaplan, *Biomaterials* **2005**, *26*, 147.
[17] Y. Cao, B. Wang, *Int. J. Mol. Sci.* **2009**, *10*, 1514.
[18] S. Kapoor, S. C. Kundu, *Acta Biomater.* **2016**, *31*, 17.
[19] T. Yucel, P. Cebe, D. L. Kaplan, *Biophys. J.* **2009**, *97*, 2044.
[20] X. Wang, J. A. Kluge, G. G. Leisk, D. L. Kaplan, *Biomaterials* **2008**, *29*, 1054.
[21] U.-J. Kim, J. Park, C. Li, H.-J. Jin, R. Valluzzi, D. L. Kaplan, *Biomacromolecules* **2004**, *5*, 786.
[22] G. G. Leisk, T. J. Lo, T. Yucel, Q. Lu, D. L. Kaplan, *Adv. Mater.* **2010**, *22*, 711.
[23] M. B. Applegate, B. P. Partlow, J. Coburn, B. Marelli, C. Pirie, R. Pineda, D. L. Kaplan, F. G. Omenetto, *Adv. Mater.* **2016**, *28*, 2417.
[24] A. S. Sarac, *Prog. Polym. Sci.* **1999**, *24*, 1149.
[25] J. A. G. Barros, G. J. M. Fechine, M. R. Alcantara, L. H. Catalani, *Polymer* **2006**, *47*, 8414.
[26] G. Qin, A. Rivkin, S. Lapidot, X. Hu, I. Preis, S. B. Arinus, O. Dgany, O. Shoseyov, D. L. Kaplan, *Biomaterials* **2011**, *32*, 9231.
[27] L. Sun, S. Zhang, J. Zhang, N. Wang, W. Liu, W. Wang, *J. Mater. Chem. B* **2013**, *1*, 3932.
[28] M. J. Zhao, L. Jung, *Free Radical Res.* **1995**, *23*, 229.
[29] C. W. P. Foo, E. Bini, J. Hensman, D. P. Knight, R. V. Lewis, D. L. Kaplan, *Appl. Phys. A* **2006**, *82*, 223.
[30] A. Babuponnusami, K. Muthukumar, *J. Environ. Chem. Eng.* **2014**, *2*, 557.
[31] G. Freddi, A. Anghileri, S. Sampaio, J. Buchert, P. Monti, P. Taddei, *J. Biotechnol.* **2006**, *125*, 281.
[32] F. E. Ali, K. J. Barnham, C. J. Barrow, F. Separovic, *J. Inorg. Biochem.* **2004**, *98*, 173.
[33] A. Matsumoto, J. Chen, A. L. Collette, U.-J. Kim, G. H. Altman, P. Cebe, D. L. Kaplan, *J. Phys. Chem. B* **2006**, *110*, 21630.
[34] X. Hu, D. Kaplan, P. Cebe, *Macromolecules* **2006**, *39*, 6161.
[35] W. L. Stoppel, A. E. Gao, A. M. Greaney, B. P. Partlow, R. C. Bretherton, D. L. Kaplan, L. D. Black, *J. Biomed. Mater. Res., Part A* **2016**, *104*, 3058.
[36] N. R. Raia, B. P. Partlow, M. McGill, E. P. Kimmerling, C. E. Ghezzi, D. L. Kaplan, *Biomaterials* **2017**, *131*, 58.
[37] S. S. Leal, H. M. Botelho, C. M. Gomes, *Coord. Chem. Rev.* **2012**, *256*, 2253.
[38] D. Ji, Y.-B. Deng, P. Zhou, *J. Mol. Struct.* **2009**, *938*, 305.
[39] Q. Liu, X. Wang, X. Tan, X. Xie, Y. Li, P. Zhao, Q. Xia, *Mater. Des.* **2018**, *146*, 134.
[40] A. Matsumoto, T. Matsumoto, H. Inoue, M. Oiwa, H. Saito, *Eur. Polym. J.* **1990**, *26*, 661.
[41] A. S. Lammel, X. Hu, S.-H. Park, D. L. Kaplan, T. R. Scheibel, *Biomaterials* **2010**, *31*, 4583.
[42] N. von Wirén, S. Klair, S. Bansal, J.-F. Briat, H. Khodr, T. Shioiri, R. A. Leigh, R. C. Hider, *Plant Physiol.* **1999**, *119*, 1107.
[43] E. Orlowska, A. Roller, H. Wiesinger, M. Pignitter, F. Jirsa, R. Krachler, W. Kandioller, B. K. Keppler, *RSC Adv.* **2016**, *6*, 40238.

[44] B. D. Lawrence, Z. Pan, A. Liu, D. L. Kaplan, M. I. Rosenblatt, *Acta Biomater.* **2012**, *8*, 3732.
[45] B. D. Lawrence, J. K. Marchant, M. A. Pindrus, F. G. Omenetto, D. L. Kaplan, *Biomaterials* **2009**, *30*, 1299.
[46] M. Choi, J. W. Choi, S. Kim, S. Nizamoglu, S. K. Hahn, S. H. Yun, *Nat. Photonics* **2013**, *7*, 987.
[47] A. N. Mitropoulos, B. Marelli, C. E. Ghezzi, M. B. Applegate, B. P. Partlow, D. L. Kaplan, F. G. Omenetto, *ACS Biomater. Sci. Eng.* **2015**, *1*, 964.
[48] D. N. Rockwood, R. C. Preda, T. Yücel, X. Wang, M. L. Lovett, D. L. Kaplan, *Nat. Protoc.* **2011**, *6*, 1612.
[49] M. McGill, J. M. Coburn, B. P. Partlow, X. Mu, D. L. Kaplan, *Acta Biomater.* **2017**, *63*, 76.